Analyst

RSC Publishing

PAPER

View Article Online
View Journal | View Issue

Cite this: *Analyst*, 2013, **138**, 461

A selective amperometric sensing platform for lead based on target-induced strand release†

Feng Li,[ab] Limin Yang,[a] Mingqin Chen,[b] Peng Li[b] and Bo Tang*[a]

Received 31st August 2012
Accepted 24th October 2012

DOI: 10.1039/c2an36227a

www.rsc.org/analyst

A novel strategy for selective and sensitive amperometric detection of lead ion (Pb^{2+}) was proposed based on target-induced strand release. The underlying gold electrode was pre-modified with dendritic gold nanoparticles by direct electrodeposition to afford increased electrode surface area for immobilization of thiol group-containing capture DNA molecules. The hybridization of the capture DNA molecules with Pb^{2+}-specific aptamer molecules to form a DNA duplex, into which methylene blue was intercalated, induced measurable electrochemical signal. Upon addition of Pb^{2+}, it could specifically bind to its aptamer to form Pb^{2+}-stablized G-quadruplex and induce the aptamer strand to release from the electrode surface into solution, accompanied by the release of intercalated MB responsible for significant signal reduction. The fabricated biosensor showed a linear response to the logarithm of Pb^{2+} concentration over the range of 1.0×10^{-10} M to 1.0×10^{-7} M with a detection limit of 7.5×10^{-11} M. In addition, this strategy afforded an exquisite selectivity for Pb^{2+} against other metal ions. The excellent sensitivity and selectivity show good potential for Pb^{2+} detection in real environmental samples.

Introduction

Nowadays, heavy metal contamination has constituted a global environmental hazard due to its highly bioaccumulative nature, non-biodegradable property and high toxicity.[1] Particularly, lead is one of the most hazardous environmental pollutants that can damage various systems of the body, including the nervous system, the reproductive system and the kidneys and cause high blood pressure and anemia,[2] a variety of neurological disorders, such as convulsions, coma and even death.[3] Especially, children are more susceptible to lead exposure due to high gastrointestinal uptake and the permeable blood–brain barrier and may suffer from learning disability, mental retardation and behavioral problems.[4] Consequently, the monitoring of lead will contribute largely to food and drinking water safety and provide valuable information for the prevention and control of lead pollution.

In the past few years we have witnessed great progress in using functional nucleic acids as molecular recognition elements for the detection of metal ions.[5] Many highly sensitive and selective lead ion (Pb^{2+}) biosensors have been developed based on a Pb^{2+}-specific RNA-cleaving DNAzyme (*i.e.*, 8–17), with the cleaving event being transformed into fluorescent, colorimetric, luminescent or electrochemical signals.[6] But the relatively high synthesis cost and low stability of Pb^{2+} specific DNAzyme limit its wide application. Alternatively, Pb^{2+}-induced allosteric G-quadruplex aptamers also can serve as specific Pb^{2+} sensing elements, with the conformational change being monitored by spectrometry, naked eyes or electrochemical methods.[6a,7] Owing to the remarkable advantages of sensitivity, simplicity, low cost, rapid response and portability of electrochemical techniques, the development of electrochemical sensors for Pb^{2+} might hold great potential for facile pollutant monitoring.[8]

The target-induced strand release strategy, usually involving an aptamer DNA duplex architecture, has received ever-growing attention in recent years due to its simple and rapid detection process and improved signals in the detection of biomolecules.[9] Li *et al.* have developed a highly sensitive and selective fluorescent Pb^{2+} biosensor based on Pb^{2+}-induced disruption of the duplex structure.[10] In a typical electrochemical protocol, the pre-immobilized capture DNA hybridizes with the aptamer to form a duplex structure *via* Watson–Crick base pairing. The probe DNA or aptamer is often labeled by a redox probe and its release from the electrode or conformational change upon addition of the target usually contributes to the electrochemical signal. Compared with it, the use of label free aptamer and redox DNA indicator should be a good substitute owing to the lower cost and improved signal. The addition of the target triggers the dissociation of the duplex structure by the formation of an aptamer–target complex, leading to the diffusion of redox indicator from the electrode surface into the solution,

[a]*College of Chemistry, Chemical Engineering and Materials Science, Key Laboratory of Molecular and Nano Probes, Ministry of Education, Shandong Normal University, Jinan 250014, China. E-mail: tangb@sdnu.edu.cn; Fax: +86-531-86180017*

[b]*College of Environment and Safety Engineering, Qingdao University of Science and Technology, Qingdao 266042, PR China*

† Electronic supplementary information (ESI) available: Detailed experimental procedures and results. See DOI: 10.1039/c2an36227a

which is responsible for the reduction of the electrochemical signal.[11] To the best of our knowledge, the target-induced strand release strategy has not been used in Pb^{2+} sensing through the electrochemical technique.

Herein, a simple, sensitive and selective amperometric Pb^{2+} biosensor was proposed based on Pb^{2+}-induced allosteric G-quadruplex release. To improve the sensitivity, the gold substrate is pre-modified with dendritic gold nanoparticles (DenAu) *via* direct electrodeposition to afford an increased surface area for capture DNA immobilization. The capture DNA will hybridize with the Pb^{2+}-specific aptamer (T30695) to form a stable duplex structure. Methylene blue (MB), an aromatic heterocycle that binds to double-stranded DNA (dsDNA) *via* intercalation is used as an electrochemical hybridization indicator.[12] Upon addition of Pb^{2+}, the duplex is induced to unwind while T30695 folds into the G-quadruplex structure stabilized by Pb^{2+}. As a result, MB dissociates away from the electrode surface, leading to significant reduction of the redox signal. The selectivity and the practical application of the biosensor were also evaluated. This study essentially offers a general mode for a wide range of target biomolecules.

Experimental section

Materials

6-Mercaptohexanol (MCH) was purchased from Sigma-Aldrich. Methylene blue (MB) and all metal salts used in this study ($CoCl_2$, $CaCl_2$, $MgCl_2$, $CdCl_2$, $NiCl_2$, $MnCl_2$, $AgNO_3$, $Hg(NO_3)_2$, KCl and $Pb(NO_3)_2$) were purchased from Sinopharm Chemical Reagent Co., Ltd. (Shanghai, China). Tris–HCl buffers were prepared by mixing stock standard solutions of Tris and HCl at various pH values. All other reagents were of analytical reagent grade and used without further purification. Double distilled water (DDW) was used throughout the measurements. The oligonucleotides were synthesized by SBS Genetech Co., Ltd. (Shanghai, China). Their base sequences are listed as follows:

Capture DNA: 5′-CAC CCA CCC AC–SH-3′

T30695: 5′-GGG TGG GTG GGT GGG T-3′

Instruments

Cyclic voltammetry (CV), differential pulse voltammetry (DPV), and electrochemical impedance spectroscopy (EIS) measurements were performed with a CHI 660D electrochemical analyzer (Shanghai, China). A three-electrode system was employed with Pt wire as the auxiliary electrode, a saturated calomel electrode (SCE) as the reference electrode, and a gold (Au) electrode or modified Au electrode as the working electrode, respectively.

Preparation of the DenAu modified Au electrode

Prior to modification, the bare Au electrode was polished with 1.0, 0.3 and 0.05 μm alumina slurry, respectively. Then the electrode was rinsed thoroughly with DDW between each polishing step and ultrasonically sequentially in acetone and DDW. Electrodeposition of DenAu on the Au electrode was carried out by applying a negative potential of −1.5 V in a stationary 2.8 mM $HAuCl_4$ and 0.1 M H_2SO_4 solution (without stirring or N_2 bubbling) for 10 min.[13] After being thoroughly rinsed with DDW, the obtained electrode was denoted as DenAu/Au.

Immobilization of capture DNA, its hybridization with T30695 and binding of indicator

For immobilization of capture DNA on the DenAu modified electrode, DenAu/Au was incubated in a 1.0 μM capture DNA solution (10 mM Tris–HCl, pH 8.0) overnight at 4 °C. After being thoroughly rinsed with DDW, the electrode was blocked by immersion in 2.0 mM MCH for 30 min to hold a good orientation of capture DNA. Then the electrode was thoroughly rinsed with DDW and denoted as C/DenAu/Au. The hybridization was conducted as follows: the C/DenAu/Au was immersed in a 1.0 μM T30695 solution (20 mM Tris–HCl/20 mM NaCl, pH 8.0). The solution was heated to 90 °C for 5 min, followed by slowly cooling down to room temperature (20 °C) and then allowed for over 3 h to ensure the complete formation of the DNA duplex. The hybridized electrode was washed with DDW to remove nonspecifically bound DNA and is denoted as T–C/DenAu/Au. MB was used as a hybridization indicator in the present work. T–C/DenAu/Au was introduced into 0.2 mM MB solution (20 mM Tris–HCl, pH 7.0) and allowed for 20 min incubation under stirring at room temperature. Afterward the MB modified electrode was thoroughly rinsed with DDW and denoted as MB/T–C/DenAu/Au.

Pb^{2+}-induced strand release from the duplex *via* formation of Pb^{2+}-stablized G-quadruplex

Pb^{2+}-induced strand release from the duplex was performed by immersing MB/T–C/DenAu/Au into solutions of different concentrations of Pb^{2+} (20 mM Tris–HCl, pH 7.0) and allowed for 30 min incubation under stirring at room temperature. Subsequently, the electrode treated with Pb^{2+} was carefully rinsed with DDW and denoted as Pb^{2+}/MB/T–C/DenAu/Au. For comparison, Pb^{2+}/MB/T–C/Au was prepared following the same procedures except for electrodeposition of DenAu on the Au electrode.

Electrochemical detection

The modified electrodes obtained during stepwise modification were electrochemically characterized by using EIS, CV and DPV. EIS measurements were performed with the frequencies ranging from 10^4 to 1.0 Hz in 1.0 mM $K_3Fe(CN)_6/K_4Fe(CN)_6$ containing 0.1 M KCl. CV and DPV measurements were performed using a 20 mM Tris–HCl (20 mM NaCl, pH 7.0) solution as the supporting electrolyte.

Results and discussion

Principle of electrochemical sensing of Pb^{2+} *via* target-induced strand release

Fig. 1 depicts the electrochemical sensing of Pb^{2+} based on Pb^{2+}-induced release of G-quadruplex from a duplex. To improve the sensitivity, the electrode was firstly modified with DenAu by direct electrodeposition. Then the DenAu modified electrode

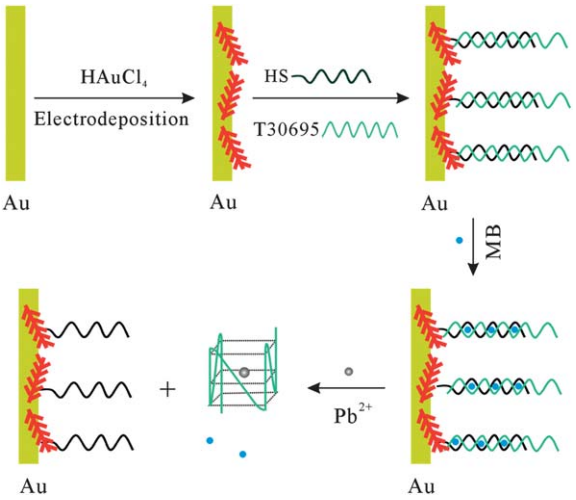

Fig. 1 Schematic illustration of Pb^{2+} detection based on target-induced strand release.

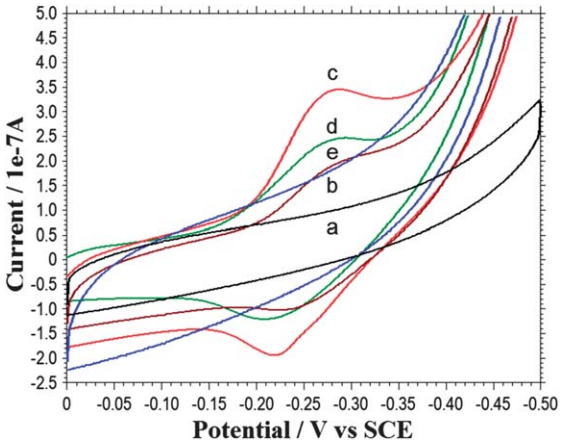

Fig. 2 CVs of C/DenAu/Au (a), T–C/DenAu/Au (b), MB/T–C/DenAu/Au (c), MB/T–C/Au (d) and Pb^{2+}/MB/T–C/DenAu/Au (e) in 20 mM Tris–HCl (20 mM NaCl, pH 7.0).

was used as the substrate for DNA immobilization and hybridization. T30695 molecule, 5′-$(GGGT)_4$-3′, can be folded into a intramolecular G-quadruplex structure in the presence of Pb^{2+}.[14] The capture DNA that is partially complementary with T30695 was self-assembled on the Au electrode surface *via* Au–S interactions. Then, the surface was subsequently blocked with MCH to form a mixed monolayer. In the absence of Pb^{2+}, T30695 molecule was hybridized with the capture DNA to form a stable duplex *via* Watson–Crick base pairing. Then MB could be intercalated into the duplex structure, resulting in a measurable electrochemical signal. However, upon addition of Pb^{2+}, the duplex dissociates owing to the formation of the G-quadruplex structure of T30695 stabilized by Pb^{2+}, followed by the release of Pb^{2+}-stabilized G-quadruplex and MB away from the electrode surface into solution, leading to significant reduction of the redox signal. Since the amount of G-quadruplex was dependent on the concentration of Pb^{2+}, the electrochemical response of MB decreased with the increasing concentration of Pb^{2+}.

Electrochemical detection

CV was preliminarily employed to follow the electrochemical response of MB before and after Pb^{2+}-induced strand release. As shown in Fig. 2, there were no redox peaks at C/DenAu/Au and T–C/DenAu/Au (Fig. 2a and b), while a pair of symmetrical redox peaks appeared at MB/T–C/DenAu/Au (Fig. 2c), with the anodic (E_{pa}) and cathodic potentials (E_{pc}) located at −0.221 V and −0.288 V, respectively. This undoubtedly corresponded to the redox behaviors of MB,[15] indicating that MB had been successfully intercalated into the duplex formed by the capture DNA and T30695. For comparison, one can observe only a relatively small redox peak at MB/T–C/Au (Fig. 2d), which further indicated that the DenAu modified electrode possessed larger active surface area than that of the bare electrode. Upon addition of Pb^{2+}, the peak current decreased dramatically (Fig. 2e), indicating that some of the surface-bound MB molecules had been liberated from the electrode into solution. It is worthy to note that MB/T–C/DenAu/Au incubated for 1 h in buffer solution containing no Pb^{2+} resulted in almost negligible decrease of the electrochemical signal (data not shown). This strongly indicated that Pb^{2+} is capable of unwinding the duplex structure *via* the formation of Pb^{2+}-stabilized G-quadruplex.

The effect of scan rates on the CV peak currents was investigated to study the electrochemical process on the electrode surface (Fig. S1†). With increasing the scan rate, E_{pa} and E_{pc} of MB on the duplex modified electrode were shifted slightly towards positive and negative potential, respectively. The peak currents were found to increase linearly to the scan rate in the range of 10 to 500 mV s^{-1}. This implied a typical surface-bound electrochemical process[16] and confirmed the intercalation of MB into the surface-bound hybrid.

EIS measurements were further performed to investigate the surface properties of modified electrodes during each preparation step (Fig. S2†). In AC impedance spectroscopy, the semicircle portion at higher frequencies corresponds to the electron-transfer limited process and the linear portion at lower frequencies ascribes to the diffusion process. The semicircle diameter equals the electron-transfer resistance (R_{et}), which depends on the dielectric and insulating features at the electrode–electrolyte interface. The electrochemical impedance spectrum of the bare electrode exhibited a small semicircle diameter (Fig. S2a†), indicating fast electron-transfer kinetics of $Fe(CN)_6^{3-}/Fe(CN)_6^{4-}$ on the bare Au electrode. However, after DenAu was electrodeposited, almost a straight line was obtained. It was probable that DenAu served as conducting wires or electron-conducting tunnels that accelerated the electron transfer rate (Fig. S2b†).[13] Then the impedance increased dramatically during the self-assembly of capture DNA molecules on the DenAu modified electrode (Fig. S2c†), due to the electrostatic repulsive force between the negatively charged phosphate bones of DNA and $Fe(CN)_6^{3-}/Fe(CN)_6^{4-}$.[17] The R_{et} value further increased after hybridization of capture DNA with T30695 (Fig. S2d†), which can be attributed to the increased negative charge of dsDNA than that of ssDNA.[18] The intercalation of MB resulted in a decreased R_{et} value (Fig. S2e†), indicating that strong electrostatic attractive

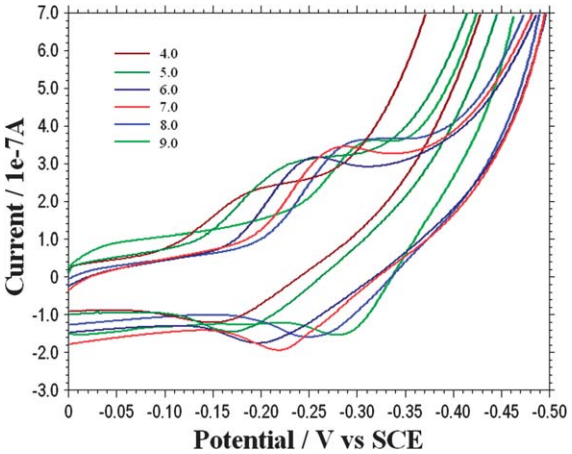

Fig. 3 CVs of MB/T–C/DenAu/Au in 20 mM Tris–HCl (20 mM NaCl) at pH values from 4.0 to 9.0.

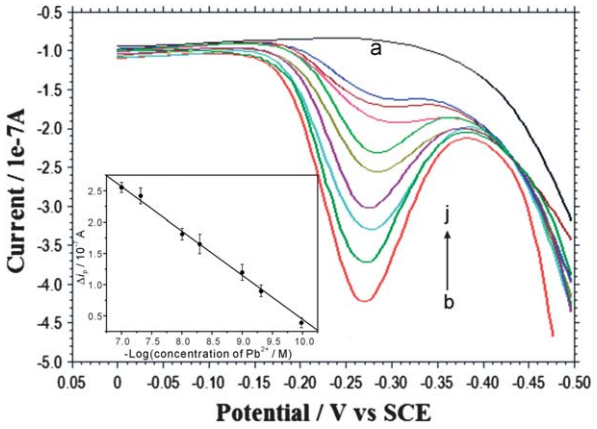

Fig. 4 DPVs of T–C/DenAu/Au (a) and MB/T–C/DenAu/Au in 20 mM Tris–HCl (20 mM NaCl, pH 7.0) with different concentrations of Pb^{2+}: 0 (b), 1.0×10^{-10} M (c), 5.0×10^{-10} M (d), 1.0×10^{-9} M (e), 5.0×10^{-9} M (f), 1.0×10^{-8} M (g), 5.0×10^{-8} M (h), 1.0×10^{-7} M (i) and 5.0×10^{-7} M (j). The inset shows the linear relationship between the DPV peak current change and the logarithm of the concentration of Pb^{2+}.

force between MB cations and $Fe(CN)_6^{3-}/Fe(CN)_6^{4-}$ made the redox couple accessible to the electrode surface. Subsequent exposure to Pb^{2+} solution induced some of the T30695 DNA molecules to release from the surface to the solution *via* the formation of Pb^{2+}-stabilized G-quadruplex,[19] which is responsible for the decreased R_{et} value.

Experimental condition optimization

The concentration of MB and the reaction time between T30695 and Pb^{2+} would have profound effects on the performance of the biosensor. The concentration of MB and the reaction time were then optimized based on the induced maximum current change. The MB signal on the dsDNA modified electrode increased rapidly with the concentration of MB up to 0.1 mM, then changed slowly, and finally reached a constant value at 0.2 mM or above (data not shown). So 0.2 mM MB was chosen as the optimum concentration. Upon exposure to 0.1 nM Pb^{2+}, the anodic peak current decreased within 30 min of incubation, and then remained constant when the reaction time was further elongated (data not shown). An incubation time of 30 min was employed as the optimum reaction time between T30695 and Pb^{2+}. Further study was performed to investigate the pH-dependence of the response of MB in the double helix. CVs of MB/T–C/DenAu/Au in 20 mM Tris–HCl (20 mM NaCl) recorded from pH 4.0 to 9.0 at a scan rate of 50 mV s^{-1} are shown in Fig. 3. The redox current increased from pH 4.0 and reached a maximum at pH 7.0. Then the current response was found to decrease from pH 7.0 to 9.0. The apparent formal potential shifted by a nearly ideal 30 mV/pH unit, indicating a reversible two electron transfer coupled with a one proton transfer electrochemical reduction process of MB over the entire pH range.[20] Since the buffer solution of pH 7.0 has the maximum signal response, 20 mM Tris–HCl (20 mM NaCl) with pH 7.0 was chosen as the supporting electrolyte.

Amperometric detection of Pb^{2+}

The binding of Pb^{2+} to T30695 DNA molecule can unwind the double helix *via* the formation of Pb^{2+}-stabilized G-quadruplex, leading to the dissociation of MB away from the electrode surface. This target induced strand release strategy was expected to give large signal change magnitude than the target-induced conformational change, in which the electrochemical events were usually recorded based on the distance alteration between the redox species and the electrode surface. Fig. 4 shows amperometric responses of MB/T–C/DenAu/Au challenged with different concentrations of Pb^{2+} under optimal conditions. When the concentration of Pb^{2+} increased from 1.0×10^{-10} M to 1.0×10^{-7} M, the current signal of MB gradually decreased, and the peak signal of the intercalated MB almost disappeared over 5.0×10^{-7} M. The inset in Fig. 4 reveals a linear correlation of the anodic current difference to the logarithm of Pb^{2+} concentration over the range of 1.0×10^{-10} M to 1.0×10^{-7} M with the relative coefficient of 0.9986. The low detection limit for Pb^{2+} was estimated to be 7.5×10^{-11} M based on 3σ. This low detection limit may be attributed to DenAu that can load more capture DNA molecules. Moreover, DenAu may serve as conducting tunnels or wires to improve the conductivity of the sensing system. The maximum contamination level for lead in drinking water defined by the U.S. Environmental Protection Agency is 72 nM, so the proposed Pb^{2+} biosensor is sufficient for Pb^{2+} monitoring in the environment. Furthermore, it exhibited better or comparable performance compared to other oligonucleotide-based biosensors through electrochemical, fluorescent or colorimetric methods.[5,6a,7b,10,21]

Selectivity and real sample detection

To confirm the binding specificity of the biosensor to Pb^{2+}, the biosensor was challenged with other metal ions. Fig. 5 shows the anodic current change of MB/T–C/DenAu/Au before and after incubation with different competing metal ions at the concentration of 1.0×10^{-7} M. It is obvious that Pb^{2+} induced the highest current decrease while most of the divalent metal ions resulted in signal decrease comparable to the blank solution. The double helix has several G residues, of which N_7 and C_6O groups

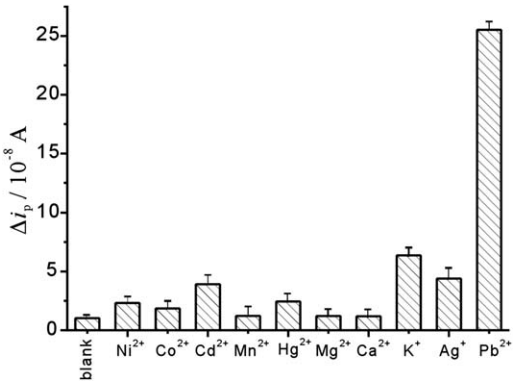

Fig. 5 Selectivity of the proposed Pb^{2+} biosensor. The concentration of Pb^{2+} and other metal ions are kept at 1.0×10^{-7} M.

may chelate with Ag^+ to form the DNA–Ag^+ complex,[22] so it is reasonable that Ag^+ resulted in a slight anodic current decrease. Except Ag^+, the current signal of MB decreased upon addition of K^+. Although K^+ is also available for G-quadruplex stabilization, Pb^{2+}-stabilized G-quadruplexes have more compact structures relative to K^+-stabilized ones.[23] Hence, Pb^{2+} induced the highest current change, indicating that the biosensor has a high selectivity toward Pb^{2+} over other tested metal ions.

The practical use of the proposed biosensor was evaluated in river water which was sampled from Laoshan Beijiushui of Qingdao. The same procedure was conducted for measurements by using river water sample instead of Pb^{2+}-containing buffer solution (Fig. S3†). MB exhibited only a very small DPV signal decrease (Fig. S3c†), which is comparable to the original signal (Fig. S3b†), indicating that the Pb^{2+} content in the tested sample is too low to be probed by the biosensor. However, there is an obvious current change in the readout signal if different concentrations of Pb^{2+} are added to the sample (Fig. S3d and e†), indicating that the proposed biosensor can be applied for the analysis of Pb^{2+} in environmental samples.

Conclusion

In this study, the strategy of target-induced strand release has been successfully utilized for sensitive and selective detection of Pb^{2+}. The three-dimensional dendritic nanostructure of DenAu was beneficial to the increased immobilization amount of capture DNA as well as the conductivity of the sensing system, which contributed to the high sensitivity of the biosensor. Meanwhile, the aptamer, T30695, with specific binding affinity for Pb^{2+} to form Pb^{2+}-stabilized G-quadruplex, endowed the biosensor with a high selectivity over other competing metal ions. This simple, facile and reliable sensing platform abrogates the tedious procedure or the use of sophisticated equipment. The excellent sensitivity and selectivity signify the potential of the biosensor for Pb^{2+} detection in real environmental samples.

Acknowledgements

This work was supported by the 973 Program (2013CB933800), the National Natural Science Foundation of China (no. 21035003, 21227005 and 21175076), the Specialized Research Fund for the Doctoral Program of Higher Education of China (20113704130001), the Program for Changjiang Scholars and Innovative Research Team in University, the Scientific Special Expenditure for Non-profit Public Industry of State Oceanic Administration (201105020), and the Science Foundation of China Postdoctoral (no. 20100471568 and 201104648).

Notes and references

1 K. Krishnani and S. Ayyappan, *Rev. Environ. Contam. Toxicol.*, 2006, **188**, 59.
2 (*a*) T. L. Guidotti and L. Ragain, *Pediatr. Clin. North Am.*, 2007, **54**, 227; (*b*) L. D. Grant, Lead and Compounds in, *Environmental Toxicants: Human Exposures and Their Health Effects*, ed. M. Lippmann, Wiley-Interscience, New York, 2009, p. 19.
3 A. D. Woolf, R. Goldman and D. C. Bellinger, *Pediatr. Clin. North Am.*, 2007, **54**, 271.
4 P. J. Landrigan, C. B. Schechter, J. M. Lipton, M. C. Fahs and J. Schwartz, *Environ. Health Perspect.*, 2002, **110**, 721.
5 (*a*) J. W. Liu and Y. Lu, *J. Fluoresc.*, 2004, **14**, 343; (*b*) B. C. Yin, B. C. Ye, W. H. Tan, H. Wang and C. C. Xie, *J. Am. Chem. Soc.*, 2009, **131**, 14624; (*c*) T. Li, L. L. Shi, E. K. Wang and S. J. Dong, *Chem.–Eur. J.*, 2009, **15**, 3347; (*d*) D. Zhang, M. G. Deng, L. Xu, Y. Y. Zhou, W. J. Yu and X. Zhou, *Chem.–Eur. J.*, 2009, **15**, 8117.
6 (*a*) C. L. Li, K. T. Liu, Y. W. Lin and H. T. Chang, *Anal. Chem.*, 2011, **83**, 225; (*b*) J. Elbaz, B. Shlyahovsky and I. Willner, *Chem. Commun.*, 2008, 1569; (*c*) X. Zhu, Z. Y. Lin, L. F. Chen, B. Qiu and G. N. Chen, *Chem. Commun.*, 2009, 6050; (*d*) Y. Xiao, A. A. Rowe and K. W. Plaxco, *J. Am. Chem. Soc.*, 2007, **129**, 262.
7 (*a*) T. Li, E. K. Wang and S. J. Dong, *Anal. Chem.*, 2010, **82**, 1515; (*b*) Z. Z. Lin, Y. Chen, X. H. Li and W. H. Fang, *Analyst*, 2011, **136**, 2367.
8 E. Palecek and M. Fojta, *Anal. Chem.*, 1994, **66**, 1566.
9 (*a*) D. Liu and S. Balasubramanian, *Angew. Chem., Int. Ed.*, 2003, **42**, 5734; (*b*) W. U. Dittmer, A. Reuter and F. C. Simmel, *Angew. Chem., Int. Ed.*, 2004, **43**, 3550; (*c*) D. S. Liu, A. Bruckbauer, C. Abell, S. Balasubramanian, D. J. Kang, D. Klenerman and D. J. Zhou, *J. Am. Chem. Soc.*, 2006, **128**, 2067.
10 T. Li, S. J. Dong and E. K. Wang, *J. Am. Chem. Soc.*, 2010, **132**, 13156.
11 (*a*) X. Zuo, S. Song, J. Zhang, D. Pan, L. Wang and C. Fan, *J. Am. Chem. Soc.*, 2007, **129**, 1042; (*b*) Z. S. Wu, M. M. Guo, S. B. Zhang, C. R. Chen, J. H. Jiang, G. L. Shen and R. Q. Yu, *Anal. Chem.*, 2007, **79**, 2933; (*c*) J. Yoshizumi, S. Kumamoto, M. Nakamura and K. Yamana, *Analyst*, 2008, **133**, 323.
12 (*a*) A. Tani, A. J. Thomson and J. N. Butt, *Analyst*, 2001, **126**, 1756; (*b*) A. Erdem, K. Kerman, B. Meric and M. Ozsoz, *Electroanalysis*, 2001, **13**, 219.
13 F. Li, X. P. Han and S. F. Liu, *Biosens. Bioelectron.*, 2011, **26**, 2619.

14 (*a*) I. Smirnov and R. H. Shafer, *J. Mol. Biol.*, 2000, **296**, 1; (*b*) P. R. Majhi and R. H. Shafer, *Biopolymers*, 2006, **82**, 558.
15 L. Zhu, R. J. Zhao, K. G. Wang, H. B. Xiang, Z. M. Shang and W. Sun, *Sensors*, 2008, **8**, 5649.
16 D. K. Gosser Jr, *Cyclic Voltammetry, Simulation and Analysis of Reaction Mechanisms*, VCH, Verlag GmbH, Weinheim, 1993.
17 F. Li, Y. Feng, P. J. Dong, L. M. Yang and B. Tang, *Biosens. Bioelectron.*, 2011, **26**, 1947.
18 Y. L. Zhou, Z. Y. Zhang, Z. N. Xu, H. S. Yin and S. Y. Ai, *New J. Chem.*, 2012, **36**, 1985.
19 F. W. Kotch, J. C. Fettinger and J. T. Davis, *Org. Lett.*, 2000, **2**, 3277.
20 D. M. Ceres, A. K. Udit, H. D. Hill, M. G. Hill and J. K. Barton, *J. Phys. Chem. B*, 2007, **111**, 663.
21 L. Shen, Z. Chen, Y. H. Li, S. L. He, S. B. Xie, X. D. Xu, Z. W. Liang, X. Meng, Q. Li, Z. W. Zhu, M. X. Li, X. C. Le and Y. H. Shao, *Anal. Chem.*, 2008, **80**, 6323.
22 R. M. Izatt, J. J. Christensen and J. H. Rytting, *Chem. Rev.*, 1971, **71**, 439.
23 F. W. Kotch, J. C. Fettinger and J. T. Davis, *Org. Lett.*, 2000, **2**, 3277.

